

**UCC Library and UCC researchers have made this item openly available.  
Please [let us know](#) how this has helped you. Thanks!**

|                                    |                                                                                                                                                                                                                                                                                                                                                                                                                  |
|------------------------------------|------------------------------------------------------------------------------------------------------------------------------------------------------------------------------------------------------------------------------------------------------------------------------------------------------------------------------------------------------------------------------------------------------------------|
| <b>Title</b>                       | Thermal stability of crystallographic planes of GaN nanocolumns and their overgrowth by metal organic vapor phase epitaxy                                                                                                                                                                                                                                                                                        |
| <b>Author(s)</b>                   | Zubialevich, Vitaly Z.; Pampili, Pietro; Parbrook, Peter J.                                                                                                                                                                                                                                                                                                                                                      |
| <b>Publication date</b>            | 2020-05-22                                                                                                                                                                                                                                                                                                                                                                                                       |
| <b>Original citation</b>           | Zubialevich, V. Z., Pampili, P. and Parbrook, P. J. (2020) 'Thermal Stability of Crystallographic Planes of GaN Nanocolumns and Their Overgrowth by Metal Organic Vapor Phase Epitaxy', <i>Crystal Growth &amp; Design</i> , 20(6), pp. 3686-3700. doi: 10.1021/acs.cgd.9b01656                                                                                                                                  |
| <b>Type of publication</b>         | Article (peer-reviewed)                                                                                                                                                                                                                                                                                                                                                                                          |
| <b>Link to publisher's version</b> | <a href="http://dx.doi.org/10.1021/acs.cgd.9b01656">http://dx.doi.org/10.1021/acs.cgd.9b01656</a><br>Access to the full text of the published version may require a subscription.                                                                                                                                                                                                                                |
| <b>Rights</b>                      | <b>This document is the Accepted Manuscript version of a Published Work that appeared in final form in <i>Crystal Growth &amp; Design</i>, copyright © American Chemical Society after peer review and technical editing by the publisher. To access the final edited and published work see <a href="https://pubs.acs.org/doi/10.1021/acs.cgd.9b01656">https://pubs.acs.org/doi/10.1021/acs.cgd.9b01656</a></b> |
| <b>Item downloaded from</b>        | <a href="http://hdl.handle.net/10468/11128">http://hdl.handle.net/10468/11128</a>                                                                                                                                                                                                                                                                                                                                |

Downloaded on 2021-11-27T15:18:18Z

# Thermal Stability of Crystallographic Planes of GaN Nanocolumns and Their Overgrowth by MOVPE

*Vitaly Z. Zubialevich<sup>1</sup>, Pietro Pampili<sup>1</sup> and Peter J. Parbrook<sup>1,2</sup>*

<sup>1</sup> Tyndall National Institute, University College Cork, T12 R5CP Cork, Ireland

<sup>2</sup> School of Engineering, University College Cork, Cork, Ireland

**Abstract:** Thermal annealing of top-down fabricated GaN nanocolumns (NCs) was investigated over a wide range of temperatures for ammonia-rich atmospheres of both nitrogen and hydrogen. It was found that in contrast to the annealing of planar GaN layers, where surface morphology change is governed purely by material decomposition, reshaping of GaN NCs is strongly affected by competition between different crystallographic facets, which in turn depends on ambient atmosphere and temperature. A qualitative mechanism explaining the observed behavior has been proposed. Based on the analysis of these annealing results, growth conditions suitable for either predominantly lateral expansion of the NCs turning their sidewalls into six well defined vertical  $m$ -plane facets, or, vice-versa, their infilling from the base regions between the NCs were determined. GaN NC arrays of increased filling factors as compared to the as top-down fabricated ones have been demonstrated using these optimized growth conditions.

## 1 Introduction

Semiconductor nanostructures are highly promising for a diversity of applications due to their large surface-to-volume ratio and quantum confinement effects that can change the essential physical properties with respect to the corresponding bulk semiconductors<sup>1</sup>. In the case of wurtzite III-nitrides,

a key material family for applications in opto- and power electronics, nanostructuring in the form of arrays of nanocolumns (NCs) has been found particularly fruitful. While there are plenty of examples for that, one perhaps most bright is worth of particular mentioning: conventional *c*-plane III-nitride based light emitters suffer from an increased radiative recombination lifetime of non-equilibrium charge carriers and a strong dependence of emission wavelength on excitation intensity due to quantum-confined Stark effect <sup>2</sup>. Using nonpolar crystallographic orientations avoids these adverse effects <sup>3</sup> but requires preparation of the corresponding heterostructures on bulk native substrates that are expensive and only available in small areas. GaN NCs oriented along the *c*-axis provide (with their sidewalls) easy alternative access to non-polar crystallographic orientations of III-nitrides <sup>4-5</sup>.

There are two main approaches to NC array fabrication: additive (bottom-up) and subtractive (top-down). While selective area growth of GaN NC arrays gives, at optimized conditions, good results in terms of crystalline quality and crystallographic faceting of prepared NCs <sup>6-7</sup>, the precise control of NC doping and dimensions (especially homogeneity of height), as well as obtaining high-density arrays without coalescence of adjacent NCs, are quite challenging. Top-down and hybrid techniques can be a promising alternative to bottom-up methods as these issues can be easily addressed this way <sup>5, 8-9</sup>. In addition to that, while the main advantage of bottom-up over the top-down approaches is the possibility to form defect-free NCs <sup>6-7</sup>, for some applications (involving core-shell structures, for instance) it is often sufficient to “bury” the pre-existing dislocations inside the NC cores.

For practical use of top-down fabricated GaN NCs, for example for nano-heterostructures with a core-shell architecture, they have to be appropriately treated to remove any surface defects introduced by the fabrication process (inductively coupled plasma etch, typically) and form well defined crystallographic facets. While for removal of plasma-induced damage, a KOH-based wet etch has been successfully implemented <sup>10-11</sup>, recovering the crystallographic facets usually requires re-growth of the top-down fabricated NCs <sup>5, 8</sup>.

Even though there have been in the past few attempts to overgrow top-down fabricated GaN NCs, a systematic study of this process has not been reported. The presence of many different crystallographic facets within NC arrays and their concave and convex surfaces makes various growth modes potentially achievable. From this point of view, the competition between different facets and how this depends on growth conditions is a particularly interesting subject. Here we investigate this by means of thermal annealing of top-down fabricated GaN NCs in ammonia-rich atmospheres of nitrogen and hydrogen.

## 2 Materials and methods

### 2.1 Object of research

We have recently developed a flexible hybrid top-down–overgrowth technique using both nanosphere and standard optical lithography for fabrication of high fill factor, (locally) ordered arrays of GaN NCs with very narrow standard deviation in their height; details of their fabrication are reported elsewhere<sup>9</sup>, but generally, the method is based closely on the procedure used previously for AlN NC arrays<sup>12-13</sup>. Such NCs, and, more specifically, the evolution of their shape during high-temperature annealing are the main objects of the current study.

As the last step of their fabrication, our GaN NCs can be left capped with protective silica disks (and residuals of silica nanospheres used as a hard mask for a dry etch into GaN) covering their top *c*-plane facets (Figure 1, *a*) or this passivation can be removed (Figure 1, *b*) using a buffered oxide etch, i.e. a mixture of hydrofluoric acid (HF) and ammonium fluoride (NH<sub>4</sub>F). GaN NCs of approximately 400 nm in diameter and 2 μm long (both capped and bare i.e. uncapped) have been studied here. The diameter of silica nanospheres used for fabrication of the studied here NCs (defines the resulting array pitch) was approximately 800 nm.

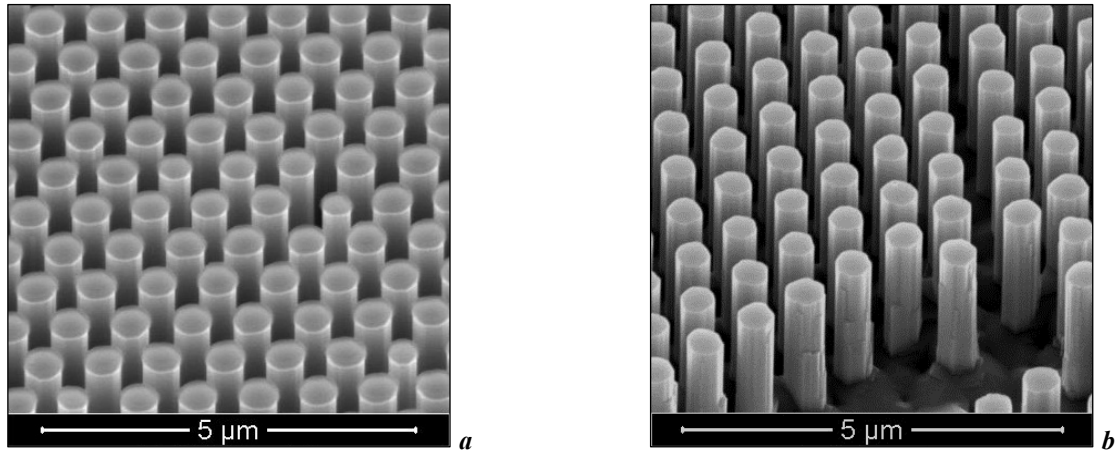


Figure 1. 45 °-tilted view of studied here SiO<sub>2</sub>-capped and (a) and uncapped (b) GaN NCs fabricated using the silica nanosphere lithography-based technique.

## 2.2 Experimental techniques

*Scanning electron microscopy* (SEM) was used to assess the original shape of GaN NCs and how it was affected by the thermal annealing. Standard high vacuum SEM was used with electron energies of 10 keV and a working distance of ~10 mm; FEI Quanta™ 650 and Carl Zeiss AG - SUPRA 40 microscopes were used to acquire the SEM pictures.

The *thermal annealing* experiments were carried out in the same 3×2” AIXTRON AG showerhead-type MOCVD reactor that was previously used to grow the initial GaN-on-sapphire epitaxial layers subsequently used for the top-down fabrication of NC arrays. The systematic annealing experiments were conducted at 300 mbar, with some additional data obtained for 400, 200 and 20 mbar. Regardless of the carrier gases used (H<sub>2</sub> or N<sub>2</sub>), the ammonia flow was 3/8 of the total flow (44.6 mmol/min). No special measures to clean the reactor before the annealing experiment was undertaken; instead, a well GaN coated susceptor was used to avoid any significant edge effects. The temperature was controlled with a thermocouple and independently monitored by two pyrometers (LayTec EpiCurveTT and Aixtron ARGUS) calibrated to show the “susceptor surface” temperature. Depending on the sample properties, this pyrometer temperature can either be essentially the susceptor pocket temperature (for smooth samples that are also optically transparent in the visible-IR spectral range), or the sample surface temperature (for opaque and/or rough samples).

In the experiments reported here, the temperatures presented are those determined by the LayTec pyrometer from a flat single-side polished *c*-plane GaN-on-sapphire wafer co-loaded with the GaN NC samples. The differences between the two independent pyrometers were within 5°C.

The *epitaxial overgrowth* of as top-down fabricated GaN NCs with nitrogen carrier gas was carried out under conditions identical to those for annealing but with a precursor (trimethylgallium, TMGa) flow of 100  $\mu\text{mol}/\text{min}$ , which respectively corresponds to V/III ratio of 446 (as compared to >1000 for typical 2D growth of GaN epilayers by MOCVD).

### 2.3 Theoretical consideration

A system of basic balance equations was used to formulate the problem mathematically and to better understand the observed temperature evolution of GaN NCs' shape. In the simplified model used here, the processes of separation of Ga atoms from the lattice (decomposition), their reincorporation to the lattice, accumulation of "free" Ga atoms (in the form of a monolayer) on the surface (adatoms) and their irreversible evaporation to the ambient environment (desorption) were considered. The first two processes were regarded separately for polar *c*-plane and non-polar *m*-plane surfaces (all other crystallographic orientations were ignored). The rates of Ga-atom leaving the GaN lattice (to become Ga adatoms on the surface) and their irreversible desorption from it were both assumed to be proportional to the Arrhenius factors  $e^{-E_a/k_B T}$  where  $E_a$  is the activation energy of the particular process and  $k_B T$  (the product of the Boltzmann constant and absolute temperature) is the average thermal energy of Ga-atoms. The opposite process of Ga-atom reincorporation from the surface back to the lattice is assumed to be less temperature dependent, particularly proportional to the  $1/\sqrt{T}$  factor<sup>14</sup>. Additionally, both reincorporation and desorption are assumed to happen only to the "free" Ga-atoms (adatoms) already on the surface (i.e. not directly from the lattice in the case of desorption), while leaving the lattice is possible only for Ga-atoms at lattice sites that are not covered by the "free" Ga-atoms pre-accumulated on the surface. This means that during annealing double-

and multiple layers of “free” Ga-atoms on the surface are not considered to occur significantly in the proposed model.

### 3 Results

#### 3.1 GaN NC shape evolution in H<sub>2</sub>+NH<sub>3</sub> ambient

While an H<sub>2</sub>+NH<sub>3</sub> atmosphere at a given temperature is usually considered to be a more aggressive environment to GaN than that of N<sub>2</sub>+NH<sub>3</sub><sup>15</sup>, we have observed only marginal reshaping of our SiO<sub>2</sub>-capped GaN NCs up to the highest studied temperature (1100°C). There is however one feature that distinguishes capped NCs annealed at the highest temperature (Figure 2, *i*) from those unannealed (Figure 1, *a*) or annealed at lower temperatures (Figure 2, *a*, *c*, *e*, and even *g*): their sidewalls start to shape hexagonally, although without any significant change in NC diameter.

Even the uncapped NCs did not reshape significantly for  $T_{\text{anneal}}$  as high as 1000°C (Figure 2, *d*). However, from  $T_{\text{anneal}}$  of about 900°C (not shown), small semipolar (although rather not crystallographically perfect) facets appeared at the intersections between the *c*-plane top facets and the non-polar sidewalls (see e.g. inset in Figure 2, *d*). The area of the semipolar facets increases slightly as  $T_{\text{anneal}}$  reaches 1000°C, while there was overall no significant change in NC shape within this temperature range (comp. Figure 2, *b* and *d*).

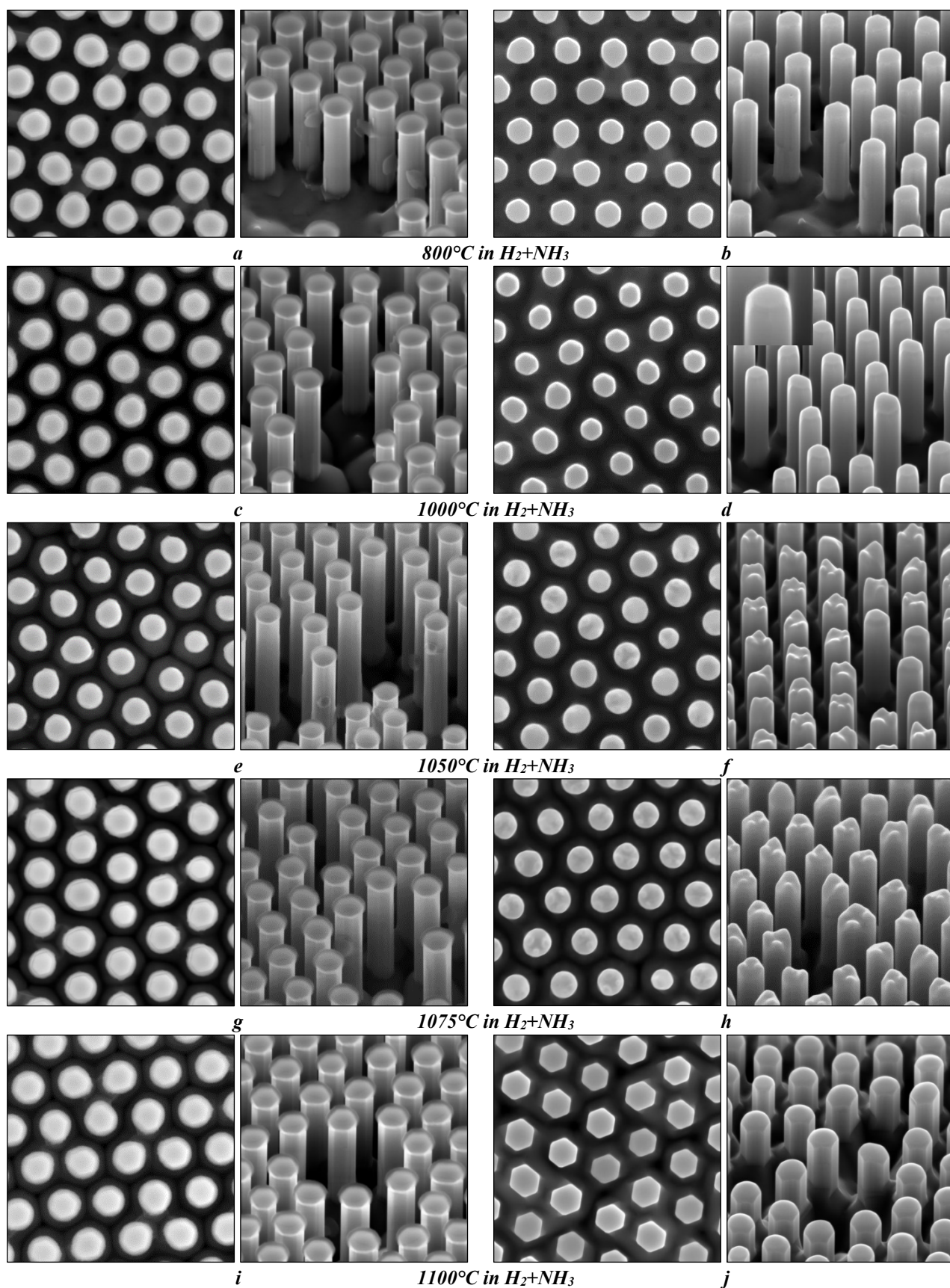


Figure 2. Top and 45° tilted views of capped (*a, c, e, g, i*) and uncapped (*b, d, f, h, j*) NCs annealed in hydrogen/ammonia atmosphere for 10 min. at 800°C (*a, b*), 1000°C (*c, d*), 1050°C (*e, f*), 1075°C (*g, h*), and 1100°C (*i, j*). The width of all pictures is 4  $\mu\text{m}$ .



At higher temperatures ( $T_{\text{anneal}} > 1000^{\circ}\text{C}$ ), unprotected top  $c$ -plane facets are observed to begin to deteriorate (roughen) more significantly. It is visible already at  $1050^{\circ}\text{C}$  (Figure 2, *f*) where only some rare NCs could preserve their original  $c$ -plane facets. At  $1075^{\circ}\text{C}$  (Figure 2, *h*), no NCs with original  $c$ -plane facets survived while their sidewalls still do not show any obvious change. Only at  $T_{\text{anneal}} = 1100^{\circ}\text{C}$ , do the sidewalls transform to six well-defined  $m$ -planes while the NCs substantially lose their heights and somewhat expand laterally in return (Figure 2, *j*). At the same time, the  $c$ -plane top face becomes smoother again but with a slightly convex profile. It is worth noting that as seen from Figure 2 and more clearly from Figure 3, where the cross-sectional views of NCs annealed at two highest temperatures are presented, up to including  $1075^{\circ}\text{C}$ , the overall damage to GaN NCs is quite marginal. At  $1075^{\circ}\text{C}$ , NCs still preserve a significant part of their original height, while already only less than a half of it remains at  $1100^{\circ}\text{C}$ .

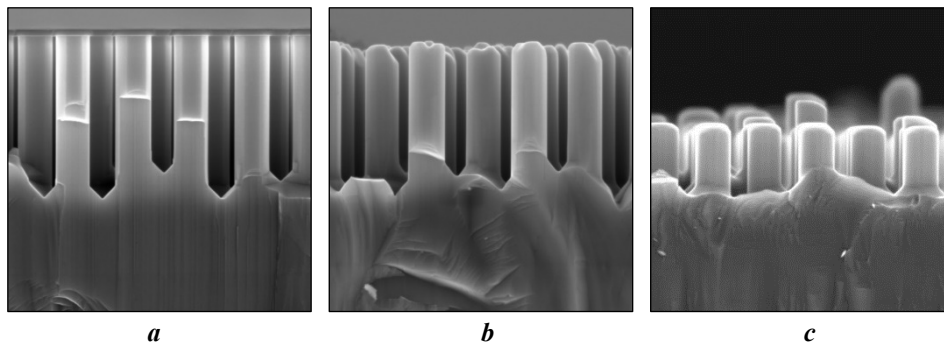


Figure 3. The cross-sectional view of capped (*a*) and uncapped (*b*, *c*) NCs upon 10 min annealing at  $1075^{\circ}\text{C}$  (*a*, *b*) and  $1100^{\circ}\text{C}$  (*c*) in  $\text{H}_2+\text{NH}_3$  atmosphere. The width of all pictures is  $4\ \mu\text{m}$ .

### 3.2 GaN NC shape evolution in $\text{N}_2+\text{NH}_3$ ambient

SEM pictures of GaN NCs annealed for 20 minutes in  $\text{N}_2+\text{NH}_3$  ambient at different temperatures in the range of  $900\text{--}1050^{\circ}\text{C}$  are presented in Figure 4. Even at relatively low-temperature conditions ( $900^{\circ}\text{C}$  – Figure 4, *a* and *b*), clear reshaping of the NCs occurs leading to their hexagonal, rather than circular cross-sections, in contrast to the  $\text{H}_2+\text{NH}_3$  atmosphere. Such a result is not completely unexpected, given our previous observation of the same mass transport in GaN NCs with a conical (truncated cone) shape at temperatures as low as  $865^{\circ}\text{C}$  when annealed in such an environment<sup>16</sup>. Substantial differences in shape evolution were found for uncapped NCs due to the

lack of protection of the top  $c$ -plane facet, exposing it to the  $N_2+NH_3$  environment and thus enabling its participation in the material mass transport. As can be seen from Figure 4, *b*, even at the lowest  $T_{\text{anneal}}$  of  $900^\circ\text{C}$ , the  $c$ -plane facet has deteriorated and become rough in remarkable contrast to the situation of  $H_2+NH_3$  presented in Figure 2 (the corresponding pictures for exactly  $900^\circ\text{C}$  in  $H_2+NH_3$  are not shown there, but one may compare Figure 4, *b* with  $800^\circ\text{C}$  and  $1000^\circ\text{C}$  cases). Similarly to the capped NCs, the uncapped ones also transform their sidewalls into six  $m$ -plane facets and the average area of the NC section becomes visibly larger.

Increasing  $T_{\text{anneal}}$  from  $900^\circ\text{C}$  to  $950^\circ\text{C}$  for the capped NCs leads to their lateral expansion in addition to well-defined  $m$ -plane facet formation (Figure 4, *c*). A dramatic increase in the average NC cross-section area is found for uncapped NCs where they lose significant fractions of their original heights (Figure 4, *d*). Notably, the resulting top surface of most of the NCs has a smooth  $c$ -plane morphology despite the ample evidence of material loss there.

Surprisingly, an increase of  $T_{\text{anneal}}$  to  $1000^\circ\text{C}$  (Figure 4, *e* and *f*) did not lead to a further continuation of the observed tendency. On the contrary, an overall decreased mass transport to NC sidewalls as compared to the case of  $950^\circ\text{C}$  is found with the capped NC profile remarkably similar to that of  $900^\circ\text{C}$  being observed (cf. Figure 4, *e* to *a*). Further increase of  $T_{\text{anneal}}$  to  $1000^\circ\text{C}$  and  $1050^\circ\text{C}$  does not lead to a stronger overall reshaping of uncapped NCs either (Figure 4, *f* and *h*). As it is seen from top views of uncapped NCs, the average cross-section area of NC annealed at these higher temperatures shows a decrease with respect to the  $950^\circ\text{C}$  case. The top facets of uncapped NCs annealed at  $1000^\circ\text{C}$  and  $1050^\circ\text{C}$ , once again, did not preserve their  $c$ -plane orientation but instead converted to irregularly oriented ones, with although broadly nanoscopically smoother morphologies than those observed for the  $900^\circ\text{C}$  annealed NCs (Figure 4, *f*, *h*).

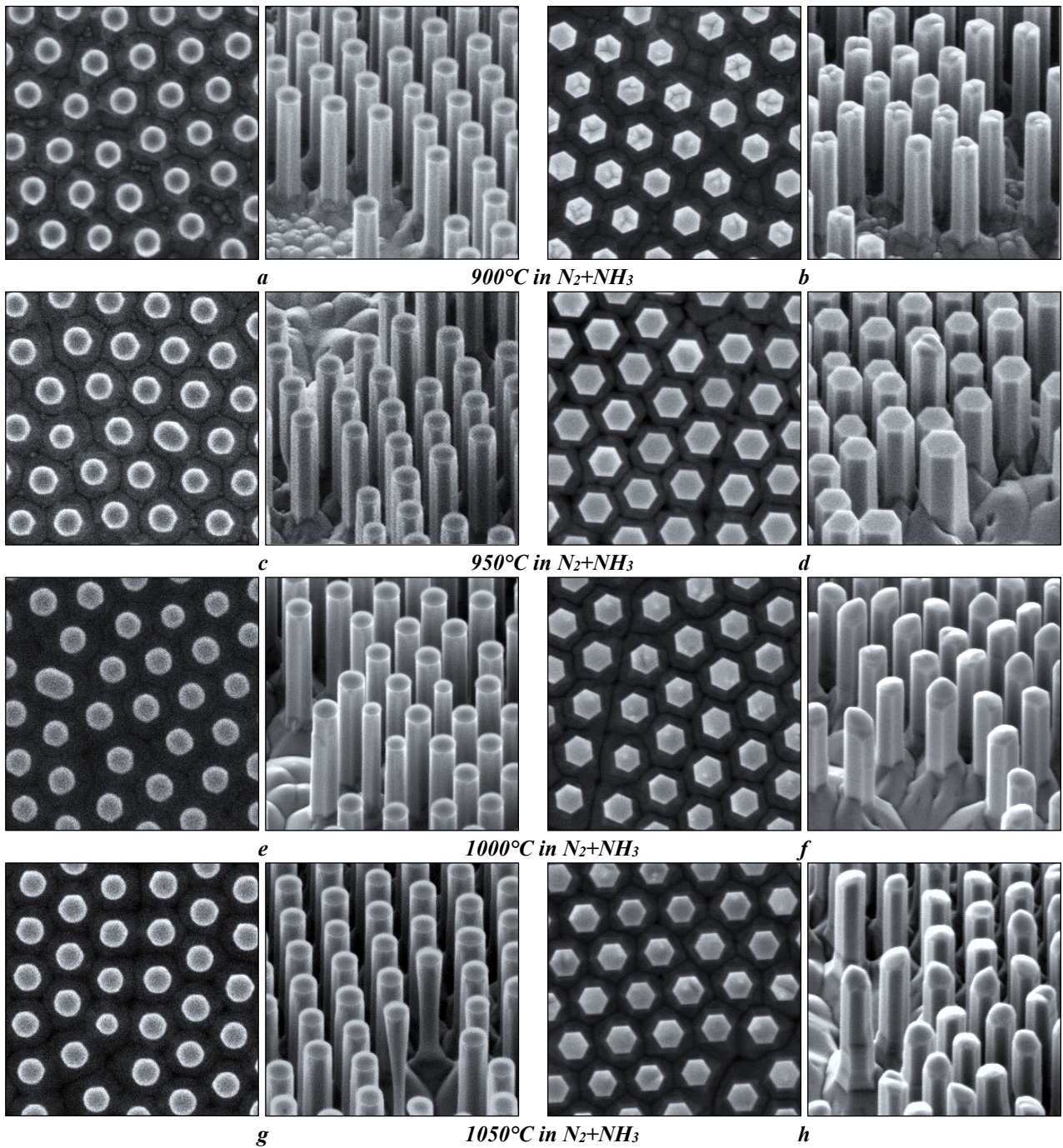


Figure 4. Top and 45° tilted views of capped (*a, c, e, g*) and uncapped (*b, d, f, h*) NCs annealed in nitrogen/ammonia atmosphere at 900°C (*a, b*), 950°C (*c, d*), 1000°C (*e, f*) and 1050°C (*g, h*). The width of all pictures is 4  $\mu\text{m}$ .

At the highest studied for this ambient  $T_{\text{anneal}}$  of 1050°C, the capped NC did not even form clear  $m$ -plane facets on their sidewalls, and, while typical NC diameter is comparable to the pre-anneal situation, some (relatively rare) NCs take on an inverse tapered shape (Figure 4, *g*). A further feature to note is that, contrary to these observations, the uncapped NCs do form  $m$ -plane facets (although

somewhat distorted and not crystallographically perfect) even at the highest studied temperature (cf. Figure 4, *g* and *h*).

Generally, uncapped NCs suffer more severely from the annealing in  $N_2+NH_3$  than the capped ones. This is manifested in the decrease of their height, increase in height variation, and stronger lateral expansion. While in the top views all GaN NCs capped with  $SiO_2$  disks “hide” completely under their caps (with the exception, perhaps, of those annealed at  $950^\circ C$  whose hexagonal sections slightly protrude out of the caps), all uncapped NCs have cross-sections that would expand out of the same apertures quite visibly.

In addition to the data above, we have undertaken an initial examination of the effect of total reactor pressure variation at an annealing temperature of  $950^\circ C$ . It is found that the NC reshaping becomes progressively faster as the pressure decreases from 400 to 200 mbar. However, at an extremely low pressure of 20 mbar (the lowest pressure achievable in our system for a total flow of 2670 sccm applied during the annealing experiments) almost no NC reshaping happens irrespective of whether ammonia is supplied. In this final case, we attempted to reproduce the selective area sublimation technique of Damilano et al.<sup>17</sup> on a larger scale (sub-micro as opposed to nano) and in the conditions of an MOCVD reactor, as opposed to the MBE setup in their original study. As the temperature in our experiment was already  $50^\circ C$  higher than in their report, the main reason for no visible GaN sublimation in our case is perhaps an insufficiently low pressure. The pressure effect on material redistribution/sublimation in GaN NC arrays is an area needing further investigation.

#### **4 Discussion**

The probability of nitrogen atoms to leave the GaN lattice is much higher than that of gallium ones at the studied temperatures<sup>18</sup>. At the same time, however, due to the presence of sufficient concentration of active nitrogen species in the ambient (3/8 of the atmosphere is ammonia with the residue being  $N_2$  or  $H_2$  as discussed earlier) during annealing, it is believed that the GaN surface should be saturated with nitrogen most likely in the form of  $NH_2$  radicals<sup>19</sup>. We, therefore, consider

the observed mass transfer to be defined not by nitrogen but gallium atoms. To understand the observed behavior, it is convenient to start from the annealing in the  $N_2+NH_3$  atmosphere.

#### 4.1 Annealing in $N_2+NH_3$ atmosphere

First of all, both capped and uncapped NCs annealed in nitrogen at  $1050^\circ C$  do not lose their material significantly. In fact, the capped ones have fixed height, and their average diameter (with marginal exceptions) does not appear to change. The uncapped NCs reduce in height although this is compensated by their lateral expansion. From this, we can conclude that the net decomposition of GaN and desorption of resulting free Ga adatoms from NC surface to the ambient at 300 mbar are both relatively weak, even at the highest applied temperature. This is in contrast with the results of the study of GaN decomposition in vacuum <sup>20</sup>, but in line with the observed effect of reduced decomposition rate due to the presence of active nitrogen <sup>21-22</sup>.

The fraction of lattice Ga atoms on the GaN surface that have enough energy to leave the lattice (and thus become free to migrate Ga adatoms however still bound to the surface) increases with temperature. As a result, they can be either reincorporated into the lattice (in another location of the same or even another facet) due to the presence of active nitrogen, or irreversibly leave the surface for the ambient. As the desorption to ambient was agreed above to be relatively weak, the observed mass transfer has to be defined by the rates of decomposition and growth at different facets (crystallographic orientations) present in the GaN NC array. From this point of view, it is clear why the overall material redistribution intensifies with an initial increase of temperature from  $900^\circ C$  to  $950^\circ C$ , but its further saturation and even inhibition is less obvious.

##### 4.1.1 Mathematical model of material transport

To understand the observed mass transport and particularly why there appears to be an optimal temperature where it is most efficient (Figure 4, *c* and *d*), a simplified mathematical model is proposed. Here the processes of Ga atom detachment (GaN decomposition) and reincorporation (GaN growth) from and to the GaN lattice (separately for the polar top NC face and the non-polar sidewall

NC faces), free Ga adatom accumulation on the NC surface, and their desorption from it are considered. The initial equation to be solved can be formulated as follows:

$$\frac{dN_c}{dt} + \frac{dN_m}{dt} = N_{S,0} \frac{d\eta_{Ga}}{dt} + \frac{dN_A}{dt}, \quad (1)$$

where  $dN_c/dt$  and  $dN_m/dt$  are the rates of GaN decomposition (or growth if negative) at the nominal  $c$ - and  $m$ -planes,  $d\eta_{Ga}/dt$  is the rate of Ga coverage change (ratio of lattice sites occupied with free Ga atoms on the surface to the total number of sites  $N_{S,0}$ ), and  $dN_A/dt$  is the rate of surface desorption to the ambient, respectively. Equation (1) basically states that the sum of rates of Ga adatom accumulation on the surface and their desorption to the ambient is equal to the sum of rates of net GaN decomposition (formation of free surface Ga adatoms) at the NCs' tops and sidewalls.

At a fixed temperature ( $dT/dt = 0$ ), it can be assumed that the surface coverage of free Ga adatoms  $\eta_{Ga}$  is constant (i.e.  $d\eta_{Ga}/dt = 0$ ) as this case corresponds to a steady-state condition. Taking this into account and explicitly expressing the particular processes as described in section 2.3, equation (1) can be expanded as follows:

$$A_c(1 - \eta_{Ga}(T))e^{-\frac{E_c}{k_B T}} - \frac{B_c}{\sqrt{T}}\eta_{Ga}(T) + A_m(1 - \eta_{Ga}(T))e^{-\frac{E_m}{k_B T}} - \frac{B_m}{\sqrt{T}}\eta_{Ga}(T) = C\eta_{Ga}(T)e^{-\frac{E_A}{k_B T}}, \quad (2)$$

where the terms  $A_i \cdot (1 - \eta_{Ga}(T)) \cdot \exp(-E_i/k_B T)$  and  $B_i \cdot \eta_{Ga}(T)/\sqrt{T}$  ( $i = c, m$ ) correspond, respectively, to the decomposition of GaN and the reincorporation of Ga adatoms from the GaN surface back to the GaN lattice at different NC facets. The term  $C \cdot \eta_{Ga}(T) \cdot \exp(-E_A/k_B T)$  describes Ga adatom desorption from the GaN surface to the ambient. The particular expressions for these processes are clear from the explanations provided in section 2.3 above.  $A_i$ ,  $B_i$  and  $C$  are empirical parameters working together with activation energies  $E_i$  to describe total probabilities (rates) of particular processes and their temperature dependencies. In particular, in the case of  $A_i$ ,  $B_i$ , the constants contain the total areas of the corresponding NC facets.

The equation (2) can be easily solved first for the Ga-atom coverage  $\eta_{Ga}(T)$ :

$$\eta_{Ga}(T) = \frac{A_c \cdot e^{-E_c/(k_B T)} + A_m \cdot e^{-E_m/(k_B T)}}{A_c \cdot e^{-E_c/(k_B T)} + A_m \cdot e^{-E_m/(k_B T)} + B_c/\sqrt{T} + B_m/\sqrt{T} + C \cdot e^{-E_A/(k_B T)}}, \quad (3)$$

which then allows individual calculation of the rates  $dN_c/dt$ ,  $dN_m/dt$ ,  $dN_A/dt$  and their analysis. The only problem is that all of the constants in expression (3) are not known. Moreover, we do not have quantitative data that would allow quantitative estimation of these constants. However, this is not the focus of this analysis, which is to check if such a model is capable of reproducing a maximum in the temperature dependence of the mass transport, and if it can, to understand what conditions need to be satisfied for this, and how feasible they are.

It was found that it is relatively easy (in a wide range of parameters) to get a negative  $dN_m/dt$  with a minimum (which corresponds to a maximum in material redistribution), if the desorption rate  $dN_A/dt$  is not insignificant. This, however, contradicts our earlier assumption that it is marginal in the case of the  $N_2$ -based atmosphere, even at the highest studied temperature. Additionally, in such cases, it would not be possible to predict the observed reduction of  $c$ -plane degradation at temperatures above the optimum. We found, however, that if parameters of GaN decomposition at  $m$ - and  $c$ -planes have the following relations:  $A_m/A_c \sim 10^4$ ,  $E_m - E_c \sim 1$  eV i.e. that GaN decomposition from the  $m$ -planes increases much faster with temperature but starts only at higher temperatures, then quite obvious peaks in both  $-dN_m/dt$  and  $dN_c/dt$  rates can be achieved even with a relatively weak desorption rate  $dN_A/dt$  (Figure 5). In the example presented in Figure 5, to position the peak at about 950°C (where the experimentally observed maximum is located) the activation energies of GaN decomposition at the  $c$ - and  $m$ -planes have to be set to about 3.0 and 3.9 eV, respectively (these values are slightly dependent on  $B_m/B_c$  ratio, which in this particular case was set to 12). Since the exact constants in the Eq. (2) are not known, the example of modeling presented in Figure 5 can serve only as a demonstrator of the possibility for the proposed model to describe a presence of the observed in the experiment maximum in the temperature dependence of material redistribution between different facets of NCs. Nevertheless, as will be shown next, it is fruitful for the understanding of what causes the observed maximum.

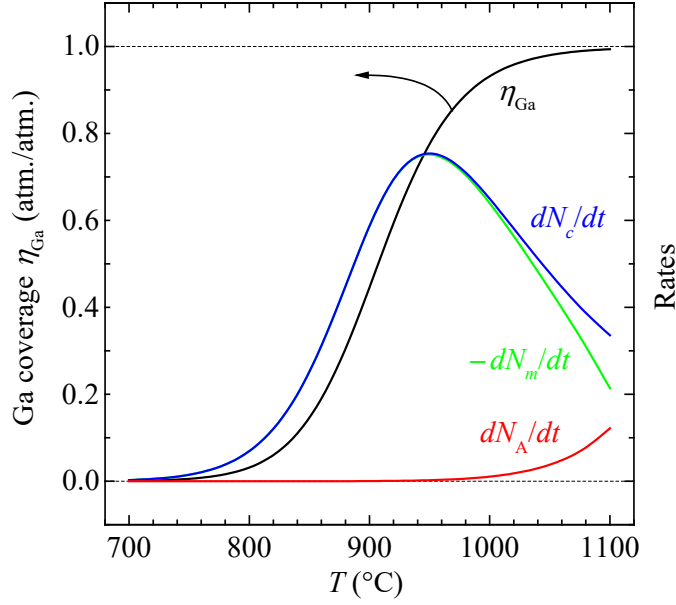


Figure 5. An example of modeling the temperature dependence of material redistribution during NC annealing in an  $N_2+NH_3$  atmosphere with equation (2), where the model can reproduce a maximum in the temperature dependence of the total mass transport.

#### 4.1.2 Mechanism of material transport at annealing in an $N_2+HN_3$ atmosphere

Based on Figure 5, we can now propose a mechanism that can qualitatively explain the behavior observed in the experiment. To understand the existence of an optimum temperature at which the total rate of material transfer maximizes, it is useful to refer to the schematic in Figure 6. Not the cause but a key parameter here is the gallium adatom coverage  $\eta_{Ga}$ , which in the schematic is represented by the thickness of NC outline (the thicker the outline the closer to unity Ga coverage). At temperatures significantly lower than  $950^\circ C$  ( $T < T_{opt}$  case in Figure 6), GaN decomposition at top  $c$ -planes is slow but faster than the local (i.e. also at  $c$ -plane facets) Ga-adatom reincorporation. Slowly degrading, the unprotected top  $c$ -planes act as a weak source of free Ga adatoms to the NC surface. GaN decomposition from the  $m$ -plane facets is not yet thermally activated at these low temperatures, and hence the net  $m$ -plane incorporation probability is very high thus making the  $m$ -plane facets an efficient sink for the Ga adatoms. With the slow Ga adatom source (top facets) and efficient sink (sidewalls), the Ga coverage  $\eta_{Ga}$  on the NC surface is low. This is why despite the high Ga adatom incorporation probability at the sidewalls the actual incorporation (and thus NC lateral



growth) is limited. The overall NC reshaping is restrained by the slow  $c$ -plane decomposition at these conditions.

At temperatures well above 950°C ( $T > T_{\text{opt}}$  case in Figure 6) in contrast, the probability of GaN decomposition from  $m$ -planes increases significantly due to its thermal activation, making the NC sidewalls a much weaker sink for the surface Ga adatoms. This can explain the slow lateral growth of NCs, but what about their vertical shrinkage due to  $c$ -plane decomposition? Indeed, at these elevated temperatures, GaN decomposition probability from the top  $c$ -plane NC facets is much stronger thermally activated as compared to the  $T < T_{\text{opt}}$  case. Top NC facets can potentially be a very efficient source of Ga adatoms in these conditions. The main cause of why they are not is the absence of efficient sinks for Ga adatoms. Slow NC lateral growth and slow Ga desorption to the ambient (this process was observed to activate only at  $T \geq 1050^\circ\text{C}$  in hydrogen, and there is no reason to consider it to be radically different here) lead to a strong accumulation of free Ga adatoms on the surface so that the coverage  $\eta_{\text{Ga}}$  approaches unity (almost continuous Ga monolayer shown with thick NC outline in  $T > T_{\text{opt}}$  case in Figure 6). NC  $c$ -plane facets are actually a weak source of free Ga adatoms in this case too, but now not due to insufficient thermal activation of the GaN decomposition probability (which was the case at  $T < T_{\text{opt}}$ ) but due significantly reduced area of GaN surface not protected by Ga adatoms. This is what limits vertical shrinkage of GaN NCs at temperatures above  $T_{\text{opt}}$  and up to until net Ga adatom desorption to the ambient gets fully thermally activated ( $T > 1050^\circ\text{C}$  judging by results of GaN NC annealing in  $\text{H}_2+\text{NH}_3$ , see below).

Unlike in the two cases above, at temperatures around 950°C ( $T_{\text{opt}}$  case in Figure 6), the  $c$ -plane facets appear to be an efficient source of free Ga atoms due to the already moderately high temperature to activate strong probability of GaN decomposition where the coverage  $\eta_{\text{Ga}}$  is still considerably lower than unity. The low  $\eta_{\text{Ga}}$  value is driven by the  $m$ -plane facets still acting as a strong sink for surface Ga adatoms as the temperature is not yet high enough to boost the GaN decomposition from the  $m$ -plane facets. At these conditions, the overall mass transport is efficient as there is a balance between how much Ga adatoms top  $c$ -plane facets can supply to the surface and

how much of them can be consumed from it by  $m$ -plane facets. In full accordance with the experimental observation (Figure 4, *d*), it leads to both a fast reduction in NC height and a proportional  $m$ -plane growth (NC lateral expansion).

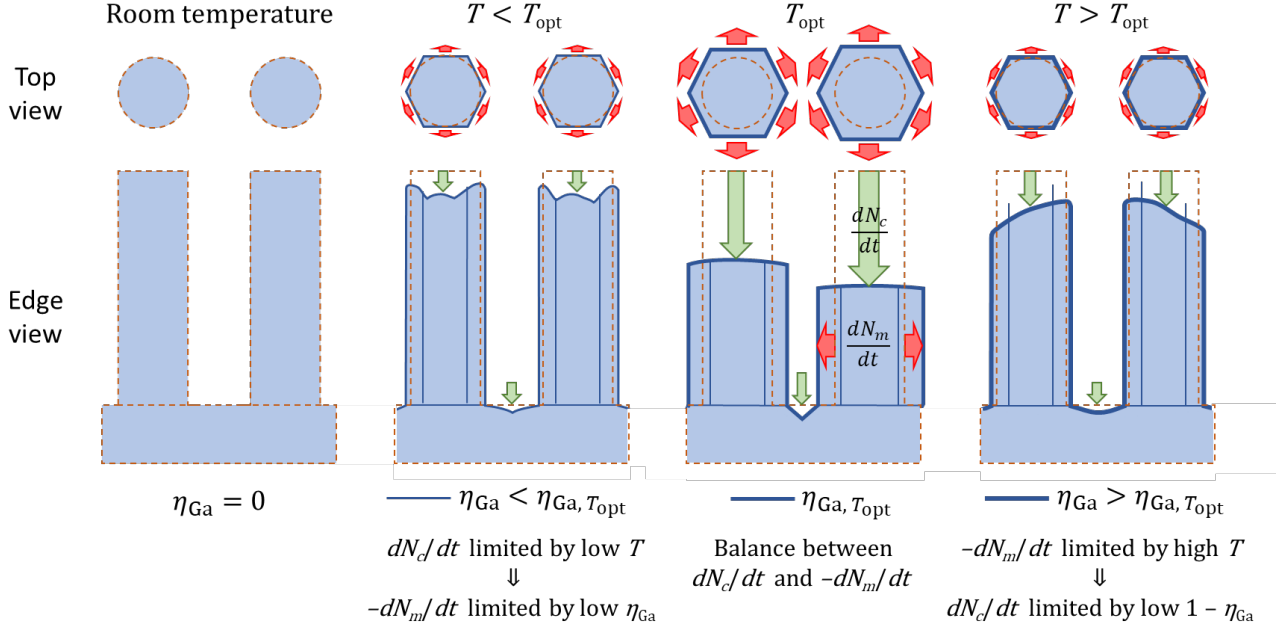


Figure 6. Schematics of shape evolution of uncapped GaN NC at different temperatures. The thickness of the NC outline graphically represents the magnitude of Ga adatom coverage.

#### 4.1.3 Reshaping of in-between NC areas and their participation in the total mass transport

Since the areas in between NCs are not passivated in our case, it is reasonable to assume that they can contribute to the mass transport to NC sidewalls too. Even capped NCs, for which Ga-adatoms cannot originate from their top  $c$ -plane facets, manage to reshape. For those annealed at 900°C and 1000°C (Figure 4, *a* and *e*, respectively), one may argue that this is material redistribution just within the sidewalls themselves (GaN decomposition at crystallographic orientations close to  $m$ -planes and Ga adatoms' reincorporation at  $a$ -planes) as it is not clear if the cross-section area changes upon reshaping. However for SiO<sub>2</sub>-capped NCs annealed at 950°C (Figure 4, *c*), it is clear that considerable lateral growth is indeed happening and so the only source of Ga-adatoms for it can be areas in between NCs.

Having said that there is a mass transport from the in-between NC areas to their sidewalls, we have to note that these regions are ultimately a weaker source of Ga adatoms in comparison to the top

*c*-plane NC facets. The fraction of the *c*-plane area blocked by SiO<sub>2</sub> capping in our array of capped NCs to the total *c*-plane area is roughly equal to the initial array fill factor (about 30%). In the case of equal efficiency of top NC facets and in-between NC areas as sources of Ga adatoms one would expect only about 30% decrease in the lateral growth for capped NCs as compared to uncapped ones. Experimentally, however, uncapped NCs expand laterally at least several times faster. Top NC facets and *c*-plane-like in-between NC regions are not thus equivalent. As soon as GaN decomposition starts, being indentations, the in-between NC regions gradually convert into concavely shaped valleys with slanted sidewalls. In ammonia-rich atmospheres, these semipolar facets are more thermally stable and thus much less suffer from further GaN decomposition<sup>23</sup>, limiting the amount of material for mass transport. For the top *c*-plane NC facets, as they are protrusions, it is difficult to convert into the same concavely shaped valleys with semipolar slopes. They try to do something similar with limited success at 900°C (see Figure 4, *b*) but this certainly does not work at  $T \geq 950^\circ\text{C}$ . One may speculate that if the annealing time was long enough, GaN decomposition at top *c*-plane NC facets would not stop until uncapped NCs are destroyed and merged while capped ones would most probably reach a stable state (after an initial expansion).

The reduced amount of material available for decomposition from the areas in-between the NC before they convert into more thermally stable (although not strictly crystallographically defined) semipolar planes and the onset of pure Ga adatoms desorption do not allow for sufficient mass transport to form well-defined *m*-planes at 1050°C (Figure 4, *g*). Even though this high temperature is not favorable for the lateral growth on NC sidewalls, an increased Ga coverage due to additional (and apparently more intense) GaN decomposition from the exposed *c*-plane tops of uncapped NCs allows for their lateral growth and formation of six *m*-plane facets (though somewhat less well defined compared to those forming at lower temperatures, Figure 4, *h*).

## 4.2 Annealing in H<sub>2</sub>+NH<sub>3</sub> atmosphere

With this general picture of what happens during annealing in the N<sub>2</sub>+NH<sub>3</sub> atmosphere, we will now consider the NC shape evolution for the annealing in H<sub>2</sub>+NH<sub>3</sub>. Although the observed “mildness” to GaN NC topology of the hydrogen atmosphere as compared to the nitrogen one seems to contradict the general knowledge regarding GaN decomposition in H<sub>2</sub> and N<sub>2</sub><sup>22, 24</sup>, this “mildness” is only “apparent”.

### 4.2.1 Stability of NC topology at temperatures below the onset of strong Ga adatom desorption

First of all, from the observed behaviors it is logical to deduce that the hydrogen-based atmosphere significantly suppresses GaN growth on nonpolar NC facets. From our data, it is also possible to conclude that this is due to their passivation by hydrogen so that they do not accept free Ga adatoms from the surface and not due to an increased GaN decomposition rate from them so that both the growth and decomposition take place and compensate each other. While the reasoning for the conclusion will be given later, it is important to point at this stage that the ultimate effect of no lateral growth is an accumulation of Ga adatoms on the surface. Originating from GaN decomposition at different facets present in NC arrays, in the absence of strong desorption ( $T < T_{\text{des}}$ ) and lateral growth, Ga adatoms do not find any sink for them and thus have to form ultimately a continuous monolayer ( $\eta_{\text{Ga}} = 1$ ) on the surface. We assume this process is happening already at temperatures below those studied here, i.e. as soon as GaN starts to decompose<sup>24</sup>. The full coverage of the GaN surfaces with a monolayer of free Ga adatoms (protective metallic film) inhibits any further decomposition and thus significant reshaping of both capped and even uncapped NCs up to 1000°C (Figure 2, *c* and *d*). This is schematically shown by the drawing in Figure 8 ( $T < T_{\text{des}}$  case) where NC outline thickness graphically represents the magnitude of Ga coverage  $\eta_{\text{Ga}}$  analogously to Figure 6.

The presence of ammonia also plays a crucial role in this protection because in its absence GaN can decompose in a hydrogen ambient at even much lower temperatures<sup>23-25</sup>. Its effect is most probably that of keeping the nitrogen atoms in their lattice positions or better to say of providing

substitutions for those that leave them. This suppresses detachment of any further Ga atoms (sitting below the surface Ga adatoms) from the lattice and thus prevents the formation of Ga droplets by keeping the amount of Ga adatoms to a monolayer. Such droplets are known to be an efficient sink of surface Ga adatoms, leading to a strong reduction of  $\eta_{\text{Ga}}$  in the adjacent areas, and a consequently enhanced GaN decomposition there <sup>25</sup>.

#### 4.2.2 Effect of thermal activation of Ga adatom desorption on NC topology

Up to about 1000°C, the desorption of free Ga adatoms from the protective film to the ambient seems to be marginal (the temperature  $T_{\text{des}}$  at which  $dN_A/dt$  becomes essentially non-zero is higher than 1000°C) and that is why no major surface morphology alterations are detectable (Figure 2, *a-d*). This changes at  $T \geq 1050^\circ\text{C}$ , when the onset of desorption immediately manifests itself in the deterioration of *c*-plane facets of uncapped NCs (Figure 2, *f*). From these observations, we can estimate the interval for  $T_{\text{des}}$  to be (1000°C, 1050°C). In the absence of lateral growth, only desorption removes free Ga adatoms from the surface. These Ga adatoms being irreversibly lost to the ambient are constantly being replenished from the bulk (thus keeping  $\eta_{\text{Ga}}$  less but close to unity), leading to the observed top facet deterioration and conversion of in-between NC areas to concavely shaped valleys with almost no *c*-plane regions there. This behavior is schematically shown in the  $T_{\text{des}} < T < T_{\text{cr}}$  case of Figure 8.

It is worth noting that the visible damage (and its nature) to only the *c*-plane-like regions and not to also NC sidewalls allows us to speculate about the higher thermal stability of non-polar and semipolar GaN orientations. Thus the reduced (or even absent) GaN decomposition at NC sidewalls cannot prevent lateral growth of NC that, considering the analogous conditions in the  $\text{N}_2+\text{HN}_3$  atmosphere, is expected to happen in the presence of both free Ga adatoms on the surface and ammonia in the ambient. Thus, not observing such growth here brings us to a conclusion of hydrogen passivation of non-polar GaN orientations similar to the one often reported for the semipolar  $\{1\bar{1}01\}$  family of planes <sup>26</sup>.

### 4.2.3 Reshaping of in-between NC areas

The mentioned above shaping of in-between NC regions into the valleys can be progressively clearer observed (by the appearance of darker and narrower regions corresponding to the intersections of adjacent slanted sidewalls) in the top-view SEMs of uncapped NCs annealed at 1000°C, 1050°C, and 1075°C (left parts of Figure 2, *d*, *f*, and *h*). This tendency seems to change for the highest annealing temperature of 1100°C though, which will be discussed later. On the other hand, for capped NCs, the valley formation appears to be complete already at 1050°C and it remains this way up to including 1100°C (left parts of Figure 2, *e*, *g* and *i*). This earlier shaping of the in-between capped NC areas can be explained by the top NC facets being the main source of Ga adatoms compensating for those irreversibly desorbed to the ambient. In the case of the unavailability of this source of Ga adatoms, i.e. when top NC facets are capped, the Ga coverage is decreased, causing a faster GaN decomposition at other *c*-plane-like regions (namely the in-between NC areas). This explanation is perfectly in line with our conclusion on a weak GaN decomposition at the NC sidewalls, which have a larger total area and are exposed to ambient in both capped and uncapped NC cases.

As discussed in 4.1.3, the in-between NC areas have a much more limited amount of material for decomposition (only until they fully convert into valleys with semipolar sidewalls) compared to the top NC facets (the latter can provide Ga adatoms as long as NCs exist). It is, therefore, logical to conjecture that in contrast to uncapped NCs, in the case of capped ones, Ga coverage decreases significantly below unity once the valley formation is complete. In these conditions, only the most thermally stable crystal orientations can survive, which may explain the better defined, i.e. almost crystallographic, valleys between capped NCs (see e.g. Figure 3, *a*).

### 4.2.4 NC reshaping at 1100°C

As can be seen from Figure 2 *i* and *j*, something radically different happens at 1100°C as compared to the tendency observed at 1000°C through 1050°C till 1075°C (almost no change in NC topology, marginal damage to the majority of NCs, and more severe but still in general marginal damage to all uncapped NCs; no visible effect on capped NCs). For capped NCs, this high

temperature and a low Ga adatom coverage induce a clear sidewall faceting as seen from their tilted view in Figure 2, *i* and more clearly from their edge view in Figure 7. As temperature increases to 1100°C, not only a strong GaN decomposition reshapes the in-between NC areas, as discussed in the previous section, but also some weak crystallographically selective GaN decomposition at NC sidewalls seems to finally start to take place too. The faceting thus happens purely by the subtractive mechanism.

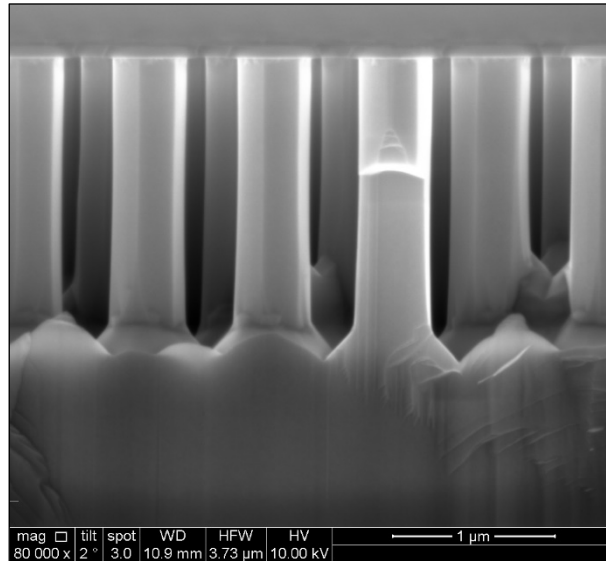


Figure 7. High magnification edge view of capped NCs annealed for 10 min at 1100°C in the  $\text{H}_2+\text{NH}_3$  atmosphere.

Much more severe reshaping of uncapped NCs takes place: they lose a significant fraction of their heights and also manage to form six reasonably well-defined *m*-plane facets (Figure 2, *j*). This lost height fraction is quite larger than the one could predict from a simple extrapolation of 1000°C, 1050°C, and 1075°C data, even taking into account the exponential (with temperature) increase of Ga adatom desorption probability as specified in Eq. (2). A lateral growth in the remained parts of uncapped NCs is obvious from their top view in Figure 2, *j* suggesting an additive mechanism of the faceting in contrast to the case of capped NCs. As both the disproportionately increased damage to NC tops and lateral (on NC sidewalls) growth do not fit into the previously described view, a change of the reshaping mechanism seems to occur at a critical temperature  $T_{cr}$  between 1075°C and 1100°C. Two plausible alternatives can be proposed to explain this observed behavior, both schematically depicted in Figure 8 ( $T > T_{cr}$  case, mechanisms 1 and 2).

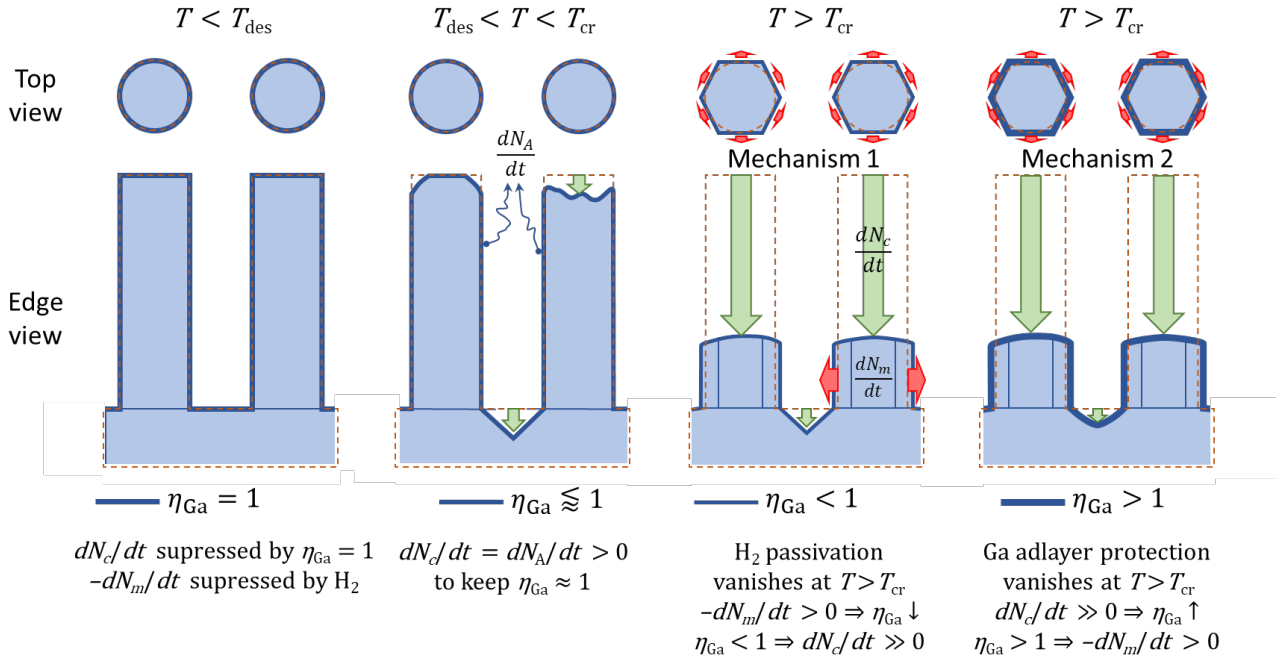


Figure 8. Schematics of shape evolution of uncapped GaN NC at different temperatures in the  $\text{H}_2 + \text{NH}_3$  ambient. The thickness of the NC outline graphically represents the magnitude of Ga adatom coverage.

The first possible mechanism lies in the temperature-induced removal of the hydrogen passivation, which was studied by Feenstra et al.<sup>26</sup> for the  $\{1\bar{1}01\}$  family of planes and, more recently, by Lymperakis et al.<sup>27</sup> for the  $m$ -plane family  $\{1\bar{1}00\}$ . This surface activation (removal of passivation) should boost free Ga adatom incorporation back into the lattice providing an additional (to Ga adatom desorption) sink for them, reducing further Ga surface coverage (Figure 8, mechanism 1 of the  $T > T_{\text{cr}}$  case). This reduction has to be, and apparently is, compensated by additional decomposition of GaN at NC top facets resulting in the fast reduction of NC height. As a result, some lateral growth and formation of six  $m$ -plane facets on the sidewalls happen as observed in the experiment, making the situation to be very similar to what happens at  $\sim 950^\circ\text{C}$  in  $\text{N}_2$ -based atmosphere. However, although plausible, this explanation leaves some uncertainties. The alleged temperature-induced activation of the surface at NC sidewalls should boost not only Ga incorporation but also a GaN decomposition there. The latter does indeed happen and, as was discussed earlier, is responsible for the faceting of capped NCs' sidewalls (Figure 2, *i* and Figure 7). On the other hand, this decomposition seems to be not very strong, and crystallographically selective. It is not clear if it



continues further upon completion of NC sidewall faceting and if the hydrogen passivation from  $m$ -planes is already removed at 1100°C. It has been recently speculated by Yoshida et al.<sup>28</sup> that the hydrogen passivation of the GaN  $m$ -plane may be still present up to above 1300°C.

The second alternative explanation lies in the assumption that, in an H<sub>2</sub>-based atmosphere, the protection from further GaN decomposition provided by the full Ga surface coverage ( $\eta_{\text{Ga}} = 1$ ) and ammonia presence gradually vanishes above a certain critical temperature  $T_{\text{cr}}$ . It does not mean though that the decomposition activates at all possible crystallographic orientations simultaneously. In our annealing in the N<sub>2</sub>-based atmosphere, it was clear that the  $c$ -plane GaN decomposition in the  $\eta_{\text{Ga}} < 1$  condition starts at a lower temperature than that at  $m$ -planes. The same is quite feasible also in the case of  $\eta_{\text{Ga}} = 1$  and H<sub>2</sub> ambient. As this *extra* decomposition rate exceeds the desorption rate of free Ga adatoms, the Ga surface coverage will start to increase (Figure 8, mechanism 2 of the  $T > T_{\text{cr}}$  case), in contrast to the case described in the previous paragraph where it was assumed to decrease instead. The excess of Ga adlayer can diffuse to the NC sidewalls and, despite the hydrogen passivation, incorporate there to form the observed  $m$ -planes. The hydrogen passivation can be removed by the substitution of hydrogen with gallium as the chemical potential difference of gallium and hydrogen increases with the rise of Ga surface coverage<sup>26</sup>.

While based on just these speculations, it is difficult to decide between the two mechanisms, there are at least two arguments in favor of the second one. First, in both these explanations, we did not so far discuss the observed net loss of material, which increased significantly at 1100°C compared to that observed at 1050°C and 1075°C. As seen from images of uncapped NCs annealed at 1100°C (Figure 3, *c*), even taking into account their slight lateral expansion, their disproportionate lowering denotes significantly increased Ga adatom desorption. While the former suggested mechanism is unable to explain this observation, the latter can account for this effect quite easily. It is known from the literature<sup>29-31</sup> that in the case of multiple layers of metallic Ga on the surface of solids, Ga atoms from the surface evaporate with activation energies corresponding to that of liquid gallium, while those from the first monolayer attached directly to the surface of solids are bonded considerably

stronger<sup>29-31</sup>. The increase of  $\eta_{\text{Ga}}$  above unity (as follows from the second proposed mechanism) thus basically reduces bonding energy of the excess Ga adatoms compared to those from the first monolayer, making the total Ga adatom desorption significantly more efficient.

For the second argument, it is useful to compare the left parts of Figure 2, *c-i* where top views of capped and uncapped NCs annealed at 1000-1100°C are presented. As discussed previously in 4.2.3, the tendency for surface reshaping in areas between the NCs to increase with the temperature seems to fail for the uncapped NCs at the highest temperature of 1100°C, while it remains strong for capped NCs at  $T \geq 1050^\circ\text{C}$ . This observation can be explained in the framework of this latter mechanism: as the Ga coverage increases above unity, the *normal* GaN decomposition (which occurs at the lattice sites unprotected by Ga adatoms) gets suppressed, leaving the *c*-plane regions between NCs less degraded. This explanation, however, requires an additional assumption regarding the *extra* GaN decomposition (occurring notwithstanding the complete Ga surface coverage). One has to assume that at least at 1100°C it occurs only (or mostly) at convexly shaped surfaces with crystallographic orientations close to *c*-plane. This assumption does not seem unreasonable<sup>14</sup>: in the case of NCs, Ga atoms located at the intersections of top *c*- and side *m*-plane facets have fewer chemical bonds with their neighbors, which makes them easier to detach from the lattice. In contrast, to start “digging” in the areas between NCs, Ga atoms from somewhere in the middle of *c*-plane regions need to be removed first (which is harder) as those at the intersections of *c*-planes with the NCs’ sidewalls have even more bonds with neighbors and should, therefore, be even harder to remove.

So, the *extra* decomposition proceeds as following: once Ga atoms at the top *c*-/side *m*-plane facets intersection are detached, the number of bonds of the neighboring atoms located next to them in the direction of the NC axis decreases making them next candidates for removal. Before this chain reaches the NC center, which corresponds to a complete stripping of one monolayer, Ga atoms at the new intersection between *c*- and *m*-planes (from the layer below) also get detached. The process easily

repeats for lower and lower layers resulting in height reduction and convexly shaped tops of 1100°C-annealed NCs, as it can be seen from their edge view (Figure 3, *c*).

It is worth noting, the wider *c*-plane regions in between uncapped NCs annealed at 1100°C are hard to explain based on the first mechanism involving temperature-induced surface activation. If the alleged thermal activation of the NC sidewall surface was the cause of the increased decomposition from their top *c*-plane facets, then the *c*-plane regions in-between uncapped NCs would be reshaped stronger. The additional sink for Ga adatoms would lower  $\eta_{\text{Ga}}$  even further below unity while temperature increases, and thus the conventional decomposition would further increase with respect to the cases of 1050°C and 1075°C, which does not seem to happen.

From the above analysis, we are thus inclined to consider the second of the two aforementioned mechanisms as the one that better describes the observed temperature surface evolution of GaN NC annealed in H<sub>2</sub>+NH<sub>3</sub> ambient at 1100°C. Further evidence in favor of this view was also obtained from NC overgrowth experiments, which are described in the next section.

## 5 NC regrowth

To understand further whether the seeming similarities in the NCs' shape evolution during annealing at 1100°C in H<sub>2</sub>+NH<sub>3</sub> atmosphere (Figure 2, *j*) and at 950°C in the N<sub>2</sub>+NH<sub>3</sub> atmosphere (Figure 4, *d*) are determined by the same mechanism or are just apparent, NC overgrowth experiments have been performed using the corresponding conditions with an additional supply of TMGa as an external source of Ga adatoms; in both cases, the overgrowth time was set to 20 min. The total thickness of GaN deposited (on a flat reference wafer) was about 440 nm during the growth in N<sub>2</sub> ambient, and is expected to be somewhat less in the case of growth in H<sub>2</sub> due to a higher desorption rate (although no growth on a flat reference wafer was undertaken in this case). The results of the two growth experiment are presented in Figure 9.

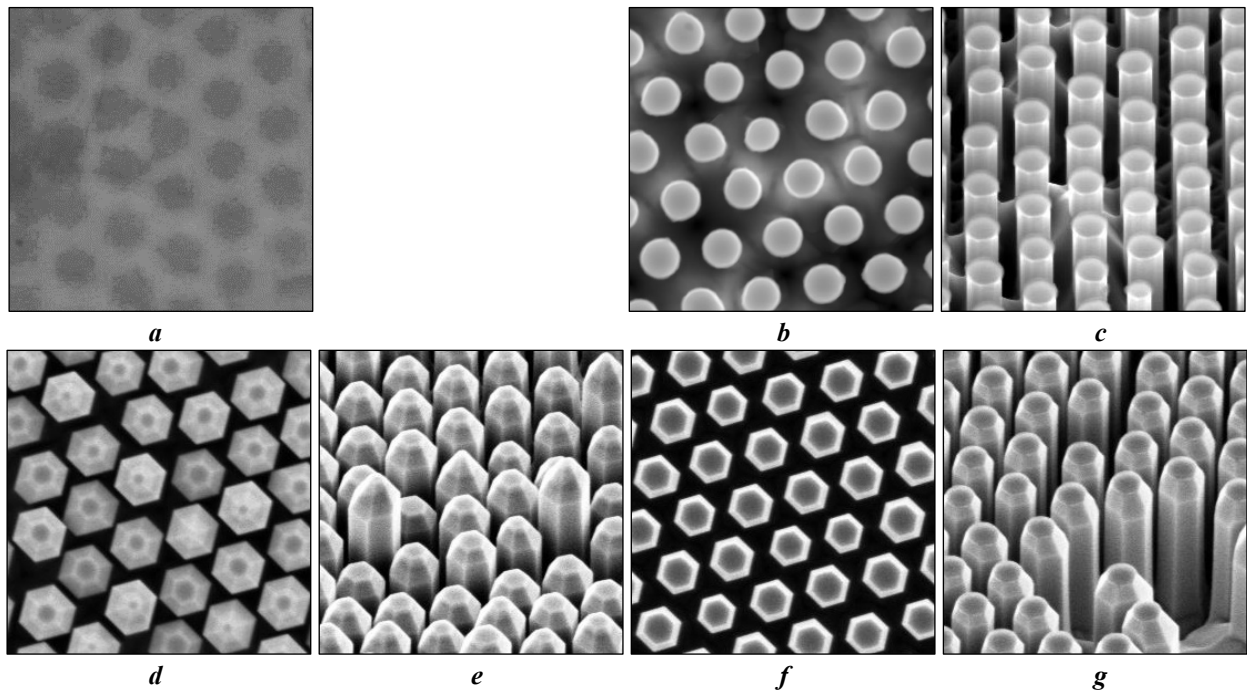


Figure 9. Top (*a, b, d, f*) and 45°-tilted (*c, e, g*) views of uncapped (*a, d, e*) and capped (*b, c, f, g*) GaN NCs overgrown for 20 min at 1100°C in the H<sub>2</sub>+NH<sub>3</sub> ambient (*a-c*) and at 950°C in the N<sub>2</sub>+NH<sub>3</sub> ambient (*d-g*).

### 5.1 Regrowth in hydrogen

As can be seen from Figure 9, *a*, uncapped GaN NCs were completely destroyed during the growth at 1100°C in H<sub>2</sub>. Some residual contrast between the regions where NCs used to be and the regions in-between them can be still seen in the top view SEM. This is believed to be due to lateral variations of conductivity (while no dopant was supplied during the regrowth step, the initial GaN epitaxial layer which NCs were formed from was Si-doped). The tilted view SEM was more sensitive to the surface topology rather than to local material conductivity; as the sample was pretty flat on this scale, the corresponding tilted view was not informative and thus omitted in Figure 9.

The fact that no NCs survived the regrowth process is partly determined by the two-times longer regrowth step in comparison to the annealing experiment. After only 10 min of annealing at 1100°C, NCs lost about 2/3 of their initial height (Figure 3 *c*) so, to some extent, it is not surprising that the 20 minutes-long annealing+overgrowth removed them completely. On the other hand, as this happened despite the external source of Ga adatoms, one has to conclude that, while contributing substantially in growth in the regions between NCs, used TMGa flowrate was not sufficient to

significantly suppress the decomposition of GaN at NC tops. This observation is in favor of the mass transfer mechanism involving thermal activation of extra GaN decomposition occurring despite the full protective metallic film ( $\eta_{\text{Ga}} \geq 1$ ) i.e. the mechanism referred to as “second” in the previous section. An external supply of Ga adatoms increases Ga coverage  $\eta_{\text{Ga}}$ , and while this is not supposed to affect the extra GaN decomposition, the conventional GaN decomposition (at sites not protected by free surface Ga adatoms) should be at least partially suppressed.

Moreover, despite the external supply of Ga adatoms, no lateral growth seems to happen at all (Figure 9, *b* and *c*) for capped NCs, which survived this long exposure to high temperature: GaN growth happens only in between the NCs instead. This fact thus allows us to completely rule out the conjecture regarding thermally induced removal of hydrogen passivation (the “first” mechanism as referred to in 4.2.4). Still, the absence of lateral growth in the case of capped NCs means that GaN decomposition at NC tops is apparently a more effective source of Ga adatoms than the external supply applied here. In this case, GaN growth in between NCs was a sufficiently strong sink for incoming Ga adatoms to keep coverage  $\eta_{\text{Ga}}$  below a threshold corresponding to the lateral growth. This implies that the lateral growth of NCs is possible even in  $\text{H}_2$  ambient if the external supply of Ga adatoms is strong enough to saturate their sink at growth sites in between NCs. On the other hand, it seems to be more useful to use these conditions ( $\text{H}_2$  atmosphere, moderate growth rate) for controlled infilling of NC array should this be necessary.

## 5.2 Regrowth in nitrogen

### 5.2.1 Optimized conditions

Unlike in the  $\text{H}_2+\text{NH}_3@1100^\circ\text{C}$  case described above, nitrogen atmosphere and moderate temperature favor lateral growth of NCs as seen from Figure 9, *d-g*. Moreover, the GaN lateral growth rate is seen from the top view SEM (Figure 9, *d* and *f*) to be noticeably higher for the uncapped NCs. While in part this is determined by the reduction of uncapped NC height, it is obvious that GaN decomposition at NC tops is the dominant source of GaN adatoms in this case too.

As is understood from the above analysis of material redistribution during annealing, the main difference in *c*-plane GaN decomposition in the cases of high temperature ( $\geq 1100^\circ\text{C}$ ) in hydrogen and moderate temperature ( $\approx 950^\circ\text{C}$ ) in nitrogen is that in the latter conditions *c*-plane GaN decomposition rate is defined by the efficiency of NC sidewalls as Ga adatoms sink. When Ga adatoms are supplied externally, the effective intensity of this sink is reduced. This is due to the competition of being incorporated onto the NC sidewalls between Ga adatoms that decompose from the NC top facets and those supplied externally. The reduced *c*-plane GaN decomposition can be understood also from Ga coverage  $\eta_{\text{Ga}}$ , which at otherwise equal conditions is increased as compared to the case of no external Ga adatom supply. The reduced *c*-plane GaN decomposition is manifested in the obvious change of NC top facet shape: truncated-pyramid-shaped apexes (Figure 9, *e*) as compared to almost perfect *c*-plane tops of uncapped NCs annealed without TMGa supply (Figure 4, *d*).

Following the logic above, besides the capping which is trivial, one of the ways to fully suppress *c*-plane GaN decomposition would be through an increase of external supply of Ga adatoms (i.e. growth rate) at least until the level at which sidewalls are capable to incorporate them without reducing Ga coverage below unity ( $\eta_{\text{Ga}} = 1$ ). An alternative way is to simply reduce the total NC sidewall area (by using low NCs and/or small NC array fill factor) at the same fixed TMGa flow. Just this approach was realized in our recent work<sup>32</sup> where at similar regrowth conditions no reduction in NC height was observed despite this may look counterintuitive at first glance.

It is interesting to note that, during regrowth at  $950^\circ\text{C}$  in nitrogen, the NC sidewall growth at the edges of an array and particularly at the sidewalls facing open areas (due to, for example, voids in the array) is significantly faster than on those located inside the array. This can be seen in the lower part of Figure 9, *g*, where (to have a good tilted view of NCs) such a place is shown, and even more clearly from Figure 10, where a top view of such a location is presented.

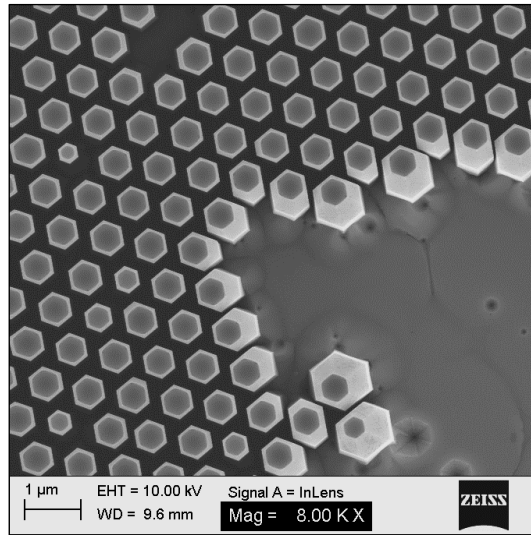


Figure 10. Top view of NCs overgrown at conditions optimized for lateral growth.

The explanation of this observation is that these conditions ( $N_2+NH_3@950^\circ C$ ) are more favorable for GaN growth on nonpolar planes as compared to  $c$ -plane. In the absence of efficient sink for Ga adatoms, local surface coverage  $\eta_{Ga}$  in the areas free of NCs is much higher (probably very close or even slightly above unity) than that inside the NC array where NC sidewalls are acting as an efficient sink. So, the NCs located at the edges of NC arrays with their sidewall facing the open areas have more Ga adatoms available to them and thus grow faster. It is worth noting that such a selective lateral growth is realized here without any intentional passivation of the  $c$ -plane areas in-between NCs. Instead, a natural  $c$ -plane “passivation” defined by the growth parameters happens and is utilized in this approach.

### 5.2.2 Effect of temperature deviation from the optimum

The temperature window for efficient lateral growth of almost perfectly vertical sidewalls without growth in-between NCs is quite narrow, though, and depends on initial NC diameter and array pitch. For NCs with an initial diameter of 100-200 nm and array pitch of 700-800 nm, it can be as narrow as  $5^\circ C (\pm 2.5^\circ C)$  and increases to about  $20^\circ C (\pm 10^\circ C)$  for NCs of 500+ nm in diameter. The following explanation can be proposed to the observed behavior: obviously, there is nothing special in the growth conditions themselves, and a flat  $c$ -plane GaN would grow normally under them. With incoming Ga adatoms but without an efficient sink for them in the form of a plurality of  $m$ -plane

facets, surface coverage  $\eta_{\text{Ga}}$  eventually exceeds unity (or a certain critical level above unity), the  $c$ -plane growth will eventually start with  $c$ -plane itself becoming a sink for them. What makes these growth conditions “special” in the case of NC arrays is exactly the presence of the plurality of nonpolar surfaces perpendicular or near-perpendicular to the  $c$ -plane, which under certain conditions are the winning competitors for incoming Ga adatoms.

To avoid growth on nominal  $c$ -plane areas in between NCs, the local Ga surface coverage  $\eta_{\text{Ga}}$  needs to be kept below a certain level, which for a given rate of external supply of Ga adatoms is equivalent to a certain rate of total Ga adatom incorporation (i.e. total efficiency of sidewalls as a Ga adatom sink). The larger total area of such surfaces per footprint is, the more efficient sink for Ga adatoms they are (under otherwise equal conditions), and thus the lower average Ga surface coverage  $\eta_{\text{Ga}}$  corresponds to the given rate of incoming Ga adatoms. For dense arrays of relatively thick (and/or high) NCs, the total area of nonpolar facets per footprint is high, and so is the total efficiency of nonpolar facets as Ga adatom sink. To reduce it below the critical level at which local  $\eta_{\text{Ga}}$  rises enough to activate the  $c$ -plane growth, a considerable deviation from the optimal conditions is required. Following the same logic, in the opposite case of sparse arrays of small NCs actual Ga surface coverage  $\eta_{\text{Ga}}$  might be already close to the value corresponding to the onset of  $c$ -plane growth even at the optimized conditions. In the latter case, even a relatively small deviation from them can trigger an undesired growth in between NCs.

### 5.2.3 Influence of NC array fill factor on regrowth perturbation due to non-optimized temperatures

While the effect of non-optimized temperature on low fill factor NC arrays usually consists of undesired growth in between NCs independently of the sign of deviation, in the case of dense NC arrays it is somewhat different. Temperatures significantly higher than the optimum induce growth in between NCs and affect the verticality of their sidewalls (making NCs wider at their bases), but lower than optimal temperatures change verticality in the opposite way so that they become wider in their upper parts instead, and no noticeable growth between NCs happens. At low temperatures ( $< 950^\circ\text{C}$ ), both non-polar and polar facets become good sinks for incoming Ga adatoms; this is the



reason of *c*-plane growth activation. Facets with *m*-plane orientation become an exceptionally good sink leading to the diffusion length of Ga adatoms on *m*-plane surfaces being considerably decreased. For dense arrays of NCs, in-between areas are quite narrow which limits direct access of incoming Ga precursor there. Due to the strong lateral flow of Ga precursor (in the gas phase) towards NC sidewalls, a gas phase gradient of Ga precursor concentration sets in along the NC length. In these conditions, almost no Ga-adatoms can reach NC foot area directly from the ambient while upper parts of NCs get considerably more Ga adatoms than their lower parts. This, together with the reduced Ga adatom diffusion length mentioned above, leads to the observed faster lateral growth of NC in their upper parts.

#### 5.2.4 Effect of hydrogen

The use of small amounts (~6%) of hydrogen as the carrier gas for TMGa source during the re-growth has an effect similar to an increase in temperature, i.e. it inhibits Ga adatom incorporation to the NC *m*-plane sidewalls, and through this it induces incorporation in the areas in between NCs. This is quite unlike the other GaN non-polar planes (*a*-planes  $\{11\bar{2}0\}$ ), whose growth is inhibited neither by the presence of hydrogen, nor by moderately high temperatures, even in the presence of *c*-planes as a competing Ga adatom sink<sup>33</sup>. The fast growth rate of *a*-planes over a wide range of parameters leads to their ultimate extinction and, in this way, defines the six *m*-plane faceted topology of GaN NC sidewalls.

This observed similarity in *m*-plane growth inhibition with adding a small amount of hydrogen, allows us to propose an alternative reason for such inhibition in pure nitrogen atmospheres at temperatures above 950°C. In our model discussed in section 4.1.1, we assumed that this effect is due to the onset of *m*-plane GaN decomposition. Our possible alternative explanation is that as temperature increases, the more efficient cracking of ammonia<sup>34</sup> provides enough hydrogen for surface passivation of the NC sidewalls. The absence of visible damage to capped NC sidewalls annealed in hydrogen (where Ga coverage is close to zero) up to at least 1050°C would be indicative of very limited *m*-plane GaN decomposition in the 950-1050°C temperature range. Whatever the

actual reason for NC sidewall growth inhibition is, the ultimate effect of it is an increase of Ga coverage due to accumulation of Ga adatoms on the surface meaning that our overall mechanism described in section 4.1.2 remains valid.

### 5.3 Growth conditions for NC infilling

By bringing the hydrogen effect to its extreme, i.e. by growing in pure H<sub>2</sub> and at moderately high temperatures, so that strong GaN decomposition at NC *c*-plane facets is not yet induced (i.e. at fairly standard conditions for planar GaN growth), it is possible to realize infilling of GaN NC arrays by regrowth. Ga adatom incorporation on sidewalls under these hydrogen-rich conditions is strongly inhibited, leading to growth being dominated by *c*-planes in between the NCs, which infills the array from bottom to top. Two examples of NC arrays with different initial fill factors are shown in Figure 11, *a* and *c*. Upon simultaneous regrowth at 1060°C and 150 mbar using H<sub>2</sub>, the array of higher fill factor is completely infilled so that the newly grown material starts to coalesce over SiO<sub>2</sub> top facet passivation of individual NCs (Figure 11, *d*). A number of pits are observed in this image, which can be attributed to incomplete coalescence due to inhomogeneities in the nanosphere lithographic array, and nanopipes formed due to small holes in the SiO<sub>2</sub> passivation of some NCs.

From examination of the array of lower initial fill factor for which NCs are only partially infilled (Figure 11, *b*), the diameter of the upper parts of NCs that remain exposed can be determined and compared to the NC diameter before regrowth. Little if any expansion of the NCs is observed in this case, indicating the growth under these conditions is dominated by that between NCs.

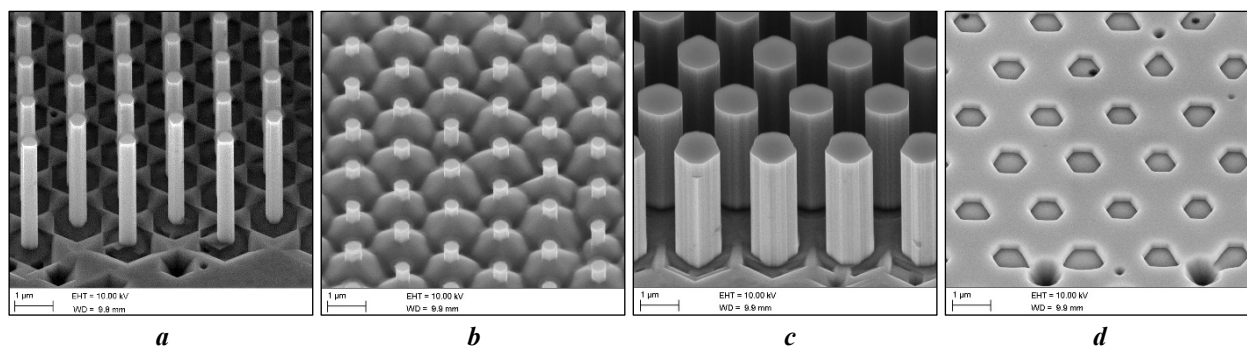


Figure 11. Examples of low (*a*) and high (*c*) fill factor arrays of SiO<sub>2</sub>-capped NCs realized by high definition conventional optical lithography, and results of their overgrowth (*b* and *d*, respectively)

with optimized for *c*-plane growth conditions (standard for planar GaN growth: H<sub>2</sub> carrier gas,  $T = 1060^\circ\text{C}$ , 150 mbar, V/III = 1200). The width of all pictures is 8  $\mu\text{m}$ .

Such growth conditions applied to arrays of GaN NCs might be useful for structures with nonplanar *p-n* junctions, for example, to realize the injection of holes to quantum wells grown around *n*-GaN NC cores in LED structures with a core-shell geometry.

## 6 Conclusions

To summarize, the thermal stability of different crystallographic orientations of GaN is studied by the analysis of annealing of GaN NC arrays (with and without SiO<sub>2</sub>-capping) in atmospheres of nitrogen and hydrogen, and in the presence of ammonia over a wide range of temperatures (800–1100°C). It was found that, unlike the case of flat *c*-plane GaN previously described in the literature, it is not the GaN decomposition and evaporation of metallic Ga that play crucial roles in the surface evolution, but the competition between different crystallographic orientations of GaN. A pure GaN sublimation (decomposition followed by evaporation of Ga adatoms) from *c*-plane facets of uncapped NCs becomes visible only at temperatures above 1000°C in hydrogen. While lower temperatures almost do not affect the shape of NCs, an increase in temperature leads to enhanced damage to the initial NC geometry. In nitrogen, in contrast, some reshaping (i.e. formation of six *m*-plane facets and deterioration of uncapped top *c*-plane facets) is clearly visible at temperatures as low as 900°C, while the overall reshaping maximizes at 950°C and decreases again at even higher temperatures.

Based on a simplified mathematical model, a qualitative mechanism that explains the observed behaviors was proposed, which takes into account thermally activated GaN decomposition, accumulation of free Ga adatoms at the surface, their reincorporation back to the lattice as well as desorption to the ambient, but ignores surface diffusion (i.e. the diffusion length was assumed to be much larger than NC dimensions). The crucial parameter driving the different scenarios was found to be the surface coverage with Ga adatoms  $\eta_{\text{Ga}}$ . In nitrogen ambient at moderately high temperatures, GaN decomposition happens on the *c*-plane only when  $\eta_{\text{Ga}}$  is lower than unity, while non-polar *m*-planes can grow at any Ga coverage above 0 if other conditions are favorable. An increase in

temperature above 950°C and a hydrogen presence are the main parameters inhibiting the net Ga adatom incorporation to *m*-planes. Their degradation as efficient sinks for Ga adatoms results in a rise of surface coverage  $\eta_{\text{Ga}}$  which in turn either slows down mass transport by suppressing GaN decomposition (during annealing) or stimulate *c*-plane growth (when Ga adatoms are supplied externally).

The understanding of the mass transport in annealed GaN arrays allowed us to identify growth conditions either inducing predominantly lateral growth on NC sidewalls, without the need of any special passivation in between NCs, or, vice-versa, forcing the material to grow only in between NCs infilling them from the bottom. Both growth modes are important for the preparation of advanced nano-heterostructures such as core-shell NCs and structures with lateral modulation of conductivity. They can be used in various optoelectronics and power electronics devices like core-shell NC-based LEDs<sup>35</sup>, solar cells<sup>36</sup>, photoelectrodes for photoelectrochemical water splitting<sup>37</sup>, and vertical Schottky diodes<sup>38</sup>.

## 7 Acknowledgments

This study was carried out with financial support from Irish Higher Education Authority Programme for Research in Third Level Institutions Cycles 4 and 5 via the INSPIRE and TYFFANI projects, from Science Foundation Ireland (through IPIC-2 and grant Nos. SFI-13/US/I2860 and SFI-18/TIDA/6066), from Tyndall National Institute (Internal Catalyst Award R18152).

## 8 References

1. Sun, C. Q., Size dependence of nanostructures: Impact of bond order deficiency. *Prog. Solid State Chem.* **2007**, *35*, 1-159.
2. Kneissl, M.; Wernicke, T., Optical and structural properties of InGaN light-emitters on non-polar and semipolar GaN. In *III-Nitride Semiconductors and their Modern Devices*, Gil, B., Ed. Oxford University Press: Oxford, 2013; pp 244-288.
3. Onuma, T.; Amaike, H.; Kubota, M.; Okamoto, K.; Ohta, H.; Ichihara, J.; Takasu, H.; Chichibu, S. F., Quantum-confined Stark effects in the *m*-plane In<sub>0.15</sub>Ga<sub>0.85</sub>N/GaN multiple quantum well blue light-emitting diode fabricated on low defect density freestanding GaN substrate. *Appl. Phys. Lett.* **2007**, *91*, 181903.

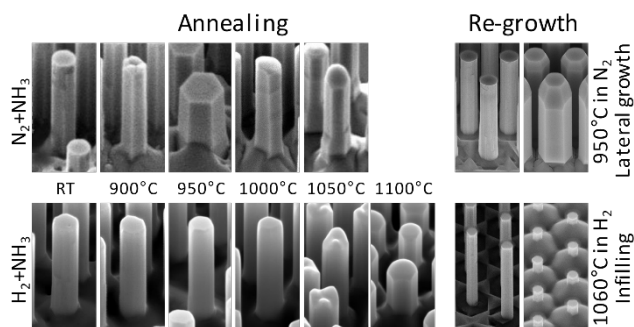
4. Yeh, T.; Stewart, L.; Chu, H.; Dapkus, P. D. In *GaN nanorods for improved light emitting diode performance*, IEEE Winter Topicals 2011, 10-12 Jan. 2011; 2011; pp 29-30.
5. Boulbar, E. D. L.; Gîrgel, I.; Lewins, C. J.; Edwards, P. R.; Martin, R. W.; Šatka, A.; Allsopp, D. W. E.; Shields, P. A., Facet recovery and light emission from GaN/InGaN/GaN core-shell structures grown by metal organic vapour phase epitaxy on etched GaN nanorod arrays. *J. Appl. Phys.* **2013**, *114*, 094302.
6. Hersee, S. D.; Sun, X.; Wang, X., The Controlled Growth of GaN Nanowires. *Nano Lett.* **2006**, *6*, 1808-1811.
7. Kishino, K.; Ishizawa, S., Selective-area growth of GaN nanocolumns on Si(111) substrates for application to nanocolumn emitters with systematic analysis of dislocation filtering effect of nanocolumns. *Nanotechnology* **2015**, *26*, 225602.
8. Chang, J.-R.; Chang, S.-P.; Li, Y.-J.; Cheng, Y.-J.; Sou, K.-P.; Huang, J.-K.; Kuo, H.-C.; Chang, C.-Y., Fabrication and luminescent properties of core-shell InGaN/GaN multiple quantum wells on GaN nanopillars. *Appl. Phys. Lett.* **2012**, *100*, 261103.
9. Zubialevich, V. Z.; Pampili, P.; McLaren, M.; Arredondo-Arechavala, M.; Sabui, G.; Shen, Z. J.; Parbrook, P. J., Dense GaN nanocolumn arrays by hybrid top-down-regrow approach using nanosphere lithography. In *2018 IEEE 18th Int. Conf. on Nanotechnology (IEEE-NANO)*, IEEE: 2018; pp 1-3.
10. Bae, S.-Y.; Kong, D.-J.; Lee, J.-Y.; Seo, D.-J.; Lee, D.-S., Size-controlled InGaN/GaN nanorod array fabrication and optical characterization. *Opt. Express* **2013**, *21*, 16854-16862.
11. Li, Q.; Westlake, K. R.; Crawford, M. H.; Lee, S. R.; Koleske, D. D.; Figiel, J. J.; Cross, K. C.; Fatholouloumi, S.; Mi, Z.; Wang, G. T., Optical performance of top-down fabricated InGaN/GaN nanorod light emitting diode arrays. *Opt. Express* **2011**, *19*, 25528-25534.
12. Conroy, M.; Zubialevich, V. Z.; Li, H.; Petkov, N.; Holmes, J. D.; Parbrook, P. J., Epitaxial lateral overgrowth of AlN on self-assembled patterned nanorods. *J. Mater. Chem. C* **2016**, *3*, 431-437.
13. Conroy, M.; Zubialevich, V. Z.; Li, H.; Petkov, N.; O'Donoghue, S.; Holmes, J. D.; Parbrook, P. J., Ultra-High-Density Arrays of Defect-Free AlN Nanorods: A "Space-Filling" Approach. *ACS Nano* **2016**, *10*, 1988-1994.
14. Miyamoto, S., A theory of the rate of sublimation. *Trans. Faraday Soc.* **1933**, *29*, 794-797.
15. Qi, Z.; Li, S.; Huang, X.; Sun, S.; Zhang, W.; Ye, W.; Dai, J.; Wu, Z.; Chen, C.; Tian, Y.; Fang, Y., Influence of high-temperature postgrowth annealing under different ambience on GaN quantum dots grown via Ga droplet epitaxy. *Opt. Mater. Express* **2015**, *5*, 1598-1605.
16. Conroy, M.; Li, H. N.; Zubialevich, V. Z.; Kusch, G.; Schmidt, M.; Collins, T.; Glynn, C.; Martin, R. W.; O'Dwyer, C.; Morris, M. D.; Holmes, J. D.; Parbrook, P. J., Self-Healing Thermal Annealing: Surface Morphological Restructuring Control of GaN Nanorods. *Cryst. Growth Des.* **2016**, *16*, 6769-6775.
17. Damilano, B.; Vézian, S.; Brault, J.; Alloing, B.; Massies, J., Selective Area Sublimation: A Simple Top-down Route for GaN-Based Nanowire Fabrication. *Nano Lett.* **2016**, *16*, 1863-1868.
18. Koleske, D. D.; Wickenden, A. E.; Henry, R. L.; DeSisto, W. J.; Gorman, R. J., Growth model for GaN with comparison to structural, optical, and electrical properties. *J. Appl. Phys.* **1998**, *84*, 1998-2010.
19. Krukowski, S.; Kempisty, P.; Jalbout, A. F., Thermodynamic and kinetic approach in density functional theory studies of microscopic structure of GaN(0001) surface in ammonia-rich conditions. *J. Chem. Phys.* **2008**, *129*, 234705.
20. Fernández-Garrido, S.; Koblmüller, G.; Calleja, E.; Speck, J. S., In situ GaN decomposition analysis by quadrupole mass spectrometry and reflection high-energy electron diffraction. *J. Appl. Phys.* **2008**, *104*, 033541.
21. Koleske, D. D.; Wickenden, A. E.; Henry, R. L., GaN Decomposition in Ammonia. *Mater. Res. Soc. Symp. Proc.* **1999**, *595*, F99W3.64.

22. Koleske, D. D.; Wickenden, A. E.; Henry, R. L.; Culbertson, J. C.; Twigg, M. E., GaN decomposition in H<sub>2</sub> and N<sub>2</sub> at MOVPE temperatures and pressures. *J. Cryst. Growth* **2001**, *223*, 466-483.
23. Coulon, P.-M.; Feng, P.; Damilano, B.; Vézian, S.; Wang, T.; Shields, P. A., Influence of the reactor environment on the selective area thermal etching of GaN nanohole arrays. *Sci. Rep.* **2020**, *10*, 5642.
24. Fathallah, W.; Boufaden, T.; El Jani, B., Analysis of GaN decomposition in an atmospheric MOVPE vertical reactor. *Phys. Status Solidi C* **2007**, *4*, 145-149.
25. Pisch, A.; Schmid-Fetzer, R., In situ decomposition study of GaN thin films. *J. Cryst. Growth* **1998**, *187*, 329-332.
26. Feenstra, R. M.; Dong, Y.; Lee, C. D.; Northrup, J. E., Recent developments in surface studies of GaN and AlN. *J. Vac. Sci. Technol., B: Microelectron. Nanometer Struct.--Process., Meas., Phenom.* **2005**, *23*, 1174-1180.
27. Lymperakis, L.; Neugebauer, J.; Himmerlich, M.; Krischok, S.; Rink, M.; Kröger, J.; Polyakov, V. M., Adsorption and desorption of hydrogen at nonpolar GaN (1-100) surfaces: Kinetics and impact on surface vibrational and electronic properties. *Phys. Rev. B* **2017**, *95*, 195314.
28. Yoshida, K.; Yamanobe, S.; Konishi, K.; Takashima, S.; Edo, M.; Monemar, B.; Kumagai, Y., Dependence of thermal stability of GaN on substrate orientation and off-cut. *Jpn. J. Appl. Phys.* **2019**, *58*, SCCD17.
29. Zheng, L. X.; Xie, M. H.; Tong, S. Y., Adsorption and desorption kinetics of gallium atoms on 6H-SiC (0001) surfaces. *Phys. Rev. B* **2000**, *61*, 4890-4893.
30. Koblmüller, G.; Averbek, R.; Riechert, H.; Pongratz, P., Direct observation of different equilibrium Ga adlayer coverages and their desorption kinetics on GaN (0001) and (000-1) surfaces. *Phys. Rev. B* **2004**, *69*, 035325.
31. Brown, J. S.; Koblmüller, G.; Averbek, R.; Riechert, H.; Speck, J. S., Quadrupole mass spectrometry desorption analysis of Ga adsorbate on AlN (0001). *J. Vac. Sci. Technol., A* **2006**, *24*, 1979-1984.
32. Zubialevich, V. Z.; McLaren, M.; Pampili, P.; Shen, J.; Arredondo-Arechavala, M.; Parbrook, P. J., Reduction of threading dislocation density in top-down fabricated GaN nanocolumns via their lateral overgrowth by MOCVD. *J. Appl. Phys.* **2020**, *127*, 025306.
33. Zheleva, T. S.; Smith, S. A.; Thomson, D. B.; Linthicum, K. J.; Rajagopal, P.; Davis, R. F., Pendeo-epitaxy: A new approach for lateral growth of gallium nitride films. *J. Electron. Mater.* **1999**, *28*, L5-L8.
34. Perman, E. P.; Atkinson, G. A. S., The Decomposition of Ammonia by Heat. *Proc. R. Soc. London* **1904**, *74*, 110-117.
35. Bavencove, A. L.; Salomon, D.; Lafossas, M.; Martin, B.; Dussaigne, A.; Levy, F.; Andre, B.; Ferret, P.; Durand, C.; Eymery, J.; Dang, L.; Gilet, P., Light emitting diodes based on GaN core/shell wires grown by MOVPE on n-type Si substrate. *Electron. Lett.* **2011**, *47*, 765-766.
36. Messanvi, A.; Zhang, H.; Neplokh, V.; Julien, F. H.; Bayle, F.; Foldyna, M.; Bougerol, C.; Gautier, E.; Babichev, A.; Durand, C.; Eymery, J.; Tchernycheva, M., Investigation of Photovoltaic Properties of Single Core-Shell GaN/InGaN Wires. *ACS Appl. Mater. Interfaces* **2015**, *7*, 21898-21906.
37. Caccamo, L.; Hartmann, J.; Fàbrega, C.; Estradé, S.; Lilienkamp, G.; Prades, J. D.; Hoffmann, M. W. G.; Ledig, J.; Wagner, A.; Wang, X.; Lopez-Conesa, L.; Peiró, F.; Rebled, J. M.; Wehmann, H.-H.; Daum, W.; Shen, H.; Waag, A., Band Engineered Epitaxial 3D GaN-InGaN Core-Shell Rod Arrays as an Advanced Photoanode for Visible-Light-Driven Water Splitting. *ACS Appl. Mater. Interfaces* **2014**, *6*, 2235-2240.
38. Sabui, G.; Zubialevich, V. Z.; White, M.; Pampili, P.; Parbrook, P. J.; McLaren, M.; Arredondo-Arechavala, M.; Shen, Z. J., GaN Nanowire Schottky Barrier Diodes. *IEEE Trans. Electron Devices* **2017**, *64*, 2283-2290.

## For Table of Contents Use Only

### Thermal Stability of Crystallographic Planes of GaN Nanocolumns and Their Overgrowth by MOVPE

Vitaly Z. Zubialevich, Pietro Pampili and Peter J. Parbrook



GaN nanocolumns preserve their topology when annealed in H<sub>2</sub>/NH<sub>3</sub> atmospheres up to 1000°C, while they reshape in N<sub>2</sub>/NH<sub>3</sub> at temperatures as low as 900°C with the strongest effect at 950°C. The apparent GaN nanocolumn H<sub>2</sub> anneal resilience is determined by suppressed reincorporation of Ga adatoms at nonpolar sidewalls, with similar suppression for N<sub>2</sub> at  $T > 950^\circ\text{C}$  explaining the observed reshaping maximum at 950°C. Selective lateral vs infilling overgrowth control can be established through the growth atmosphere choice.